

# Performance-based seismic design of reinforced concrete ductile buildings subjected to large energy demands

Amador Teran-Gilmore<sup>1\*</sup>, Alberto Sanchez-Badillo<sup>2</sup> and Marco Espinosa-Johnson<sup>1</sup>

<sup>1</sup>*Departamento de Materiales, Universidad Autónoma Metropolitana, Av. San Pablo 180,  
Col. Reynosa Tamaulipas, México 02200, D.F.*

<sup>2</sup>*Alonso y Asociados, Carretera México-Toluca 1725, Despacho C-5, Col. Lomas de Palo Alto,  
México 05110, D.F.*

*(Received October 17, 2009, Accepted February 19, 2010)*

**Abstract.** Current seismic design codes do not contemplate explicitly some variables that are relevant for the design of structures subjected to ground motions exhibiting large energy content. Particularly, the lack of explicit consideration of the cumulative plastic demands and of the degradation of the hysteretic cycle may result in a significant underestimation of the lateral strength of reinforced concrete structures built on soft soils. This paper introduces and illustrates the use of a numerical performance-based methodology for the predesign of standard-occupation reinforced concrete ductile structures. The methodology takes into account two limit states, the performance of the non-structural system, and in the case of the life safety limit state, the effect of cumulative plastic demands and of the degradation of the hysteretic cycle on the assessment of structural performance.

**Keywords:** nonlinear analysis; narrow-banded motions; stiffness degradation; ductile reinforced concrete frames; cumulative plastic demands.

---

## 1. Introduction

For a given period of vibration, the lateral strength of an earthquake-resistant structure and its level of structural damage, follow an inverse relation. Because of this, a fundamental decision made when establishing a seismic design code is the definition of strength design spectra. The specification of an insufficient lateral strength can result in excessive structural damage, and thus, in inadequate structural performance. The design spectra currently included in seismic design codes do not seem to take into account the effect of several variables that should be explicitly considered during their formulation. As a consequence, the design strength spectra ordinates may be insufficient to adequately control structural damage on reinforced concrete ductile structures subjected to ground motions exhibiting large energy content.

Several analytical studies carried out by Mexican researchers illustrate the severity of the plastic cumulative demands that are expected in structures built in the soft soil of Mexico City, and their design implications (Teran 1996, Rodriguez and Ariztizabal 1999, Huerta and Reinoso 2002,

---

\* Corresponding Author, Professor, E-mail: [tga@correo.azc.uam.mx](mailto:tga@correo.azc.uam.mx)

Bojorquez and Ruiz 2004, Arroyo and Ordaz 2007, Teran and Bahena 2007). Particularly, Teran and Jirsa (2005) suggest that the maximum deformation thresholds that have been proposed for displacement-based design methodologies (Qi and Moehle 1991, Priestley 2000) do not seem conservative enough to guarantee adequate damage control in structures located in the Lake Zone of Mexico City. Furthermore, several soft soil sites worldwide, such as the Bay Mud of the San Francisco Bay Area, have the potential to generate long-duration narrow-banded motions with high energy content (Seed and Sun 1989), in such way that seismic design of structures located in this type of soil should account for cumulative plastic demands.

This paper formulates, within the framework established for performance-based design by the Vision 2000 Committee (SEAOC 1995), a numerical design methodology for reinforced concrete frames subjected to severe plastic cumulative deformation demands. The methodology explicitly accounts for the immediate operation and life safety limit states, and makes explicit consideration of low cycle fatigue and the effect of degradation of the hysteretic cycle. The use of the methodology is illustrated through its application to the design of a 12-story building.

## 2. Low cycle fatigue

Experimental and field evidence indicates that the lateral strength, stiffness and ultimate deformation capacity of reinforced concrete structures deteriorate every time they incur in plastic behavior. A possible consequence of excessive deterioration of the hysteretic behavior of a structure is failure of critical elements at deformation levels that are significantly smaller than its ultimate deformation capacity under unidirectional loading (Teran and Jirsa 2005).

Recently, the engineering profession confronted the need to design structures with predictable performance. As a consequence, proposals for design against low cycle fatigue began focusing on deformation control rather than relying exclusively on detailing recommendations to ensure stable hysteretic behavior. A key issue during the development of design methodologies to control low cycle fatigue was the recognition that the lateral strength of a structure plays an instrumental role in controlling the seismic demands that eventually induce this type of failure.

Two low cycle fatigue models developed for reinforced concrete structures will be used herein. The first one, developed by Park and Ang (1985) has been extensively used to develop seismic design methodologies (e.g., Fajfar 1992, Bertero and Bertero 1992)

$$DMI_{PA} = \frac{\mu_{max}}{\mu_u} + \beta \frac{NE_{H\mu}}{\mu_u} \quad (1)$$

where  $\mu_{max}$  is the maximum ductility demand,  $\mu_u$  is the ultimate ductility and  $\beta$  is a structural parameter that characterizes the stability of the hysteretic behavior of the structure.  $NE_{H\mu}$  is the plastic energy (area under all the hysteresis loops a structure undergoes during the ground motion) normalized by the strength and displacement at first yield. For an elasto-perfectly-plastic system subjected to multiple plastic excursions,  $NE_{H\mu}$  is the sum of all plastic displacements reached in the different cycles normalized by the displacement at yield, in such way that it can be interpreted as a cumulative ductility (Teran and Jirsa 2005). While  $\beta$  equal to 0.15 corresponds to ductile systems that exhibit a fairly stable hysteretic behavior (Cosenza *et al.* 1993);  $\beta$  between 0.2 and 0.4

correspond to systems that exhibit important degradation of strength and stiffness (Williams and Sexsmith 1997). Under the presence of multiple cyclic deformations, 1.0 represents the threshold value of  $DMI_{PA}$  at which failure is expected to occur.

The second is a simple energy-based model developed by Terán and Jirsa (2005)

$$NE_{H_\mu} = \frac{1.5}{(2-b)}(\mu_u - 1) \quad (2)$$

where  $b$  is the structural parameter that characterizes the stability of the hysteretic cycle. The value of  $NE_{H_\mu}$  estimated from Eq. 2 establishes the plastic energy demand that a structure can accommodate before failure due to low cycle fatigue. For seismic design of ductile structures  $b = 1.5$ , in such way that

$$NE_{H_\mu} = 3(\mu_u - 1) \quad (3)$$

### 3. Effect of degradation of the hysteretic cycle

For several years, it was believed that the degradation of the hysteretic cycle had little effect on the lateral strength demands of earthquake-resistant structures (e.g., Mahin and Bertero 1981). Nevertheless, several studies suggest that, for narrow-banded long-duration motions generated in soft soils, the seismic demands in degrading systems can be significantly different than those corresponding to non-degrading systems (Terán 1996, Miranda and Ruiz-Garcia 2002). Generally, for a fundamental period of vibration ( $T$ ) less than the corner or dominant period of motion ( $T_g$ ), strength requirements in degrading systems tend to be larger than those for an elasto-plastic system. The opposite usually occurs for  $T$  larger than  $T_g$ .

This paper extends previous studies carried out in soft soils to contemplate the effect of cumulative plastic deformation demands. For such purpose, the Park and Ang damage model was used to evaluate damage in single-degree-of-freedom (SDOF) systems exhibiting elasto-perfectly-plastic behavior and the hysteretic behaviors summarized in Fig. 1. The behaviors correspond to the cyclic response of ductile reinforced concrete structures (note there is no pinching of the hysteresis loops), and were modeled using the three parameters model (Kunnath *et al.* 1990). As a reference, values of  $\alpha$  of 2 and 10 imply significant and insignificant stiffness degradation during reloading, respectively; and  $\beta$  of zero and 0.15 correspond to no strength degradation and to strength degradation typical of a ductile structure, respectively. It should be mentioned that the parameter  $\beta$  used to degrade the strength in the three parameters model has a full correspondence with that used in Eq. 1.

Fig. 2 shows the mean normalized strength spectra for constant damage ( $DMI_{PA} = 1$ ) corresponding to seven motions recorded in the Lake Zone of Mexico City and having a corner period of two seconds. These motions, which will be used to establish design spectra for the 12-story building, are summarized in Table 4.  $S_{an}$  in the figure denotes normalized strength, and corresponds to the strength demand in a degrading system normalized by that of an elasto-perfectly-plastic system having the same period, percentage of critical damping and ultimate deformation capacity. Note that if pinching is not present, the particularities of the hysteretic cycle do not affect significantly the strength demands of the degrading systems. Although not shown, it is important to point out that the values of  $S_{an}$  derived from the Park and Ang criteria are very similar to those

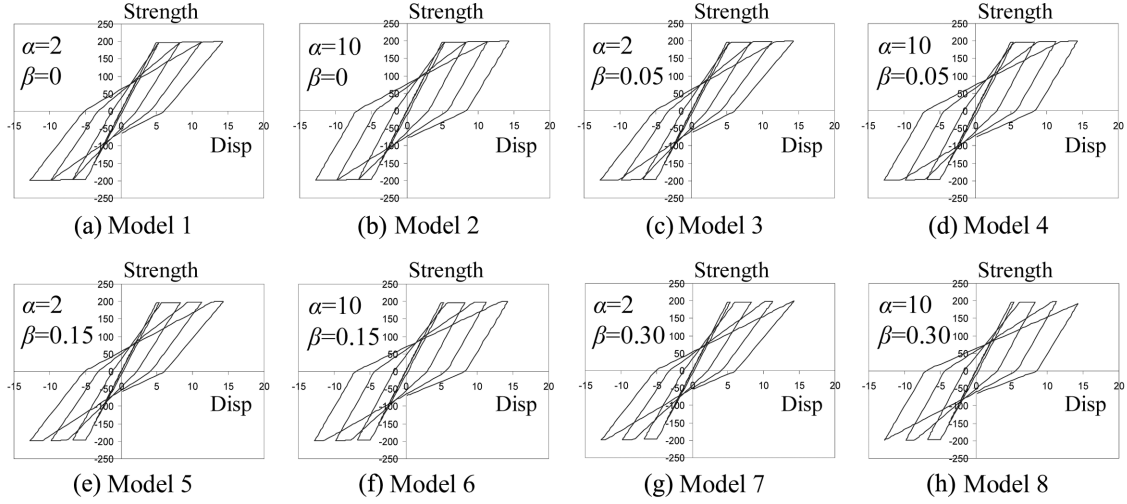
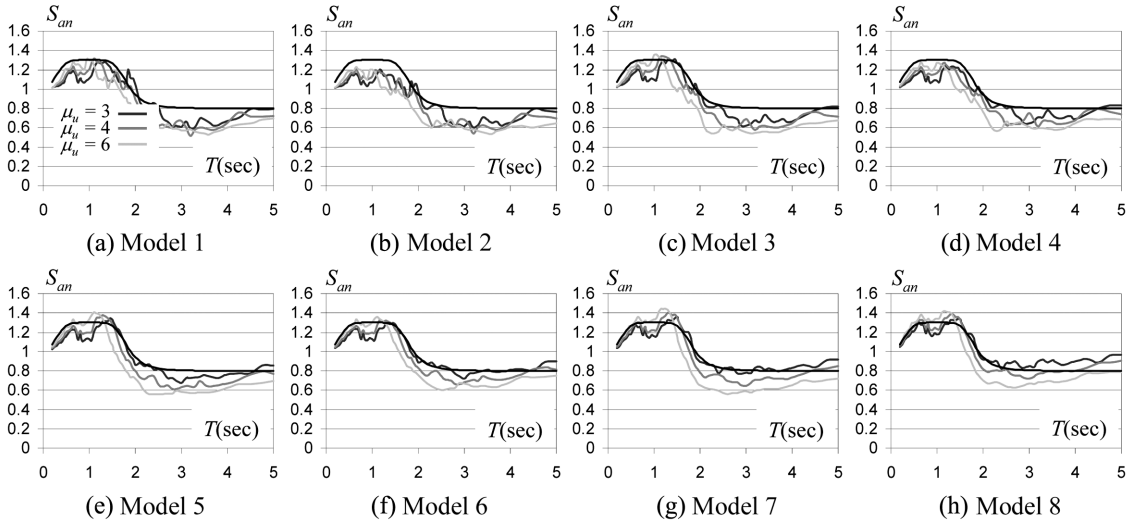


Fig. 1 Hysteretic behaviors under consideration

Fig. 2 Normalized strength spectra for constant damage ( $DMI_{PA} = 1$ ), Lake Zone of Mexico City, 5% critical damping

derived from constant maximum ductility strength spectra.

The strength in degrading systems can be estimated by modifying the strength evaluated from spectra derived from elasto-perfectly-plastic behavior according to

$$S_a^{DEG}(T, \mu_u) = S_{an} S_a^{EPP}(T, \mu_u) \quad (4)$$

where  $S_a^{DEG}(T, \mu_u)$  is the strength demand evaluated for a period  $T$  and an ultimate ductility capacity  $\mu_u$  for a degrading system; and  $S_a^{EPP}(T, \mu_u)$  is the corresponding strength for an elasto-perfectly-plastic system. From an extensive study of the strength demands in SDOF systems, the value of  $S_{an}$  corresponding to the Lake Zone of Mexico City can be estimated as

$$S_{an}(T) = \frac{1}{2 + 5 \left| \frac{T}{0.5 T_g} - 1 \right|^5} + 0.8 \quad (5)$$

Fig. 2 compares the estimates of  $S_{an}$  obtained with Eq. 5 with the actual values for this parameter corresponding to ultimate ductilities of 3, 4 and 6. Regarding the displacement demand, it is possible to formulate a similar approach

$$S_d^{DEG}(T, \mu_u) = S_{dn} S_d^{EPP}(T, \mu_u) \quad (6)$$

where  $S_d^{DEG}(T, \mu_u)$  and  $S_d^{EPP}(T, \mu_u)$  correspond to the displacement demands in the degrading and non-degrading systems, respectively, and  $S_{dn}$  is the correction factor that accounts for the effect of degradation. If the structural evaluation criteria for the structure is that of maximum ductility, the values of  $S_{an}$  and  $S_{dn}$  for a given structure are equal. Nevertheless, if a constant damage criteria (such as Park and Ang) is used, the values of  $S_{an}$  and  $S_{dn}$  can be different. Particularly, for  $DMI_{PA} = 1$ , Eq. 1 results in

$$\mu_{max} = \mu_u - \beta N E_{H\mu} \quad (7)$$

Because plastic energy demands vary from a degrading to a non-degrading system, the value of maximum ductility offered by Eq. 7 varies, as illustrated in Fig. 3, according to the type of hysteretic behavior. Under these circumstances,  $S_{dn}$  should consider the following

$$S_{dn} = \frac{S_d^{DEG}}{S_d^{EPP}} = \frac{S_{dy}^{DEG} \mu_{max}^{DEG}}{S_{dy}^{EPP} \mu_{max}^{EPP}} = \frac{S_a^{DEG} \mu_{max}^{DEG}}{S_a^{EPP} \mu_{max}^{EPP}} = S_{an} \frac{\mu_{max}^{DEG}}{\mu_{max}^{EPP}} \quad (8)$$

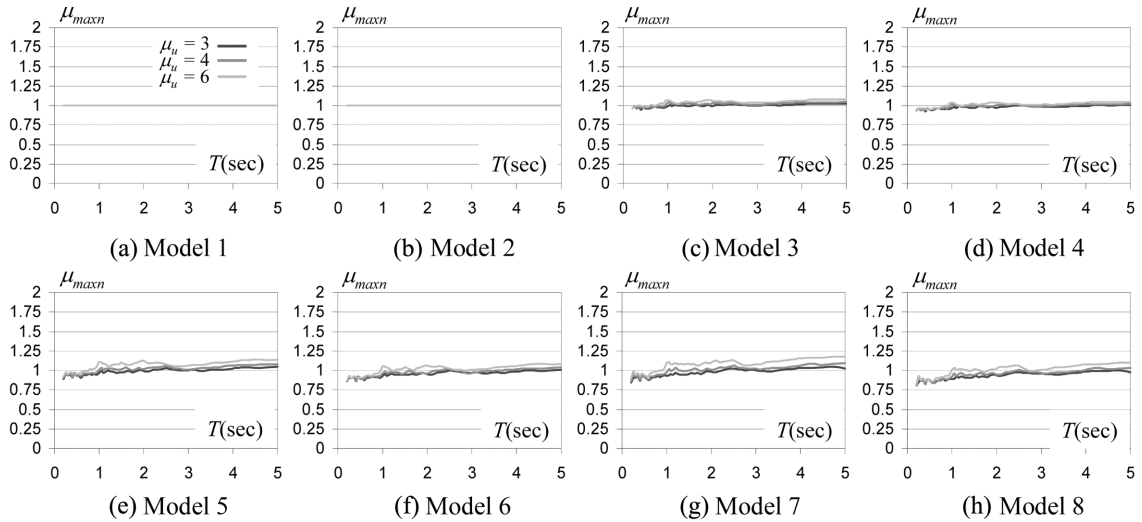


Fig. 3 Normalized maximum ductility for constant damage ( $DMI_{PA} = 1$ ), Lake Zone of Mexico City, 5% critical damping

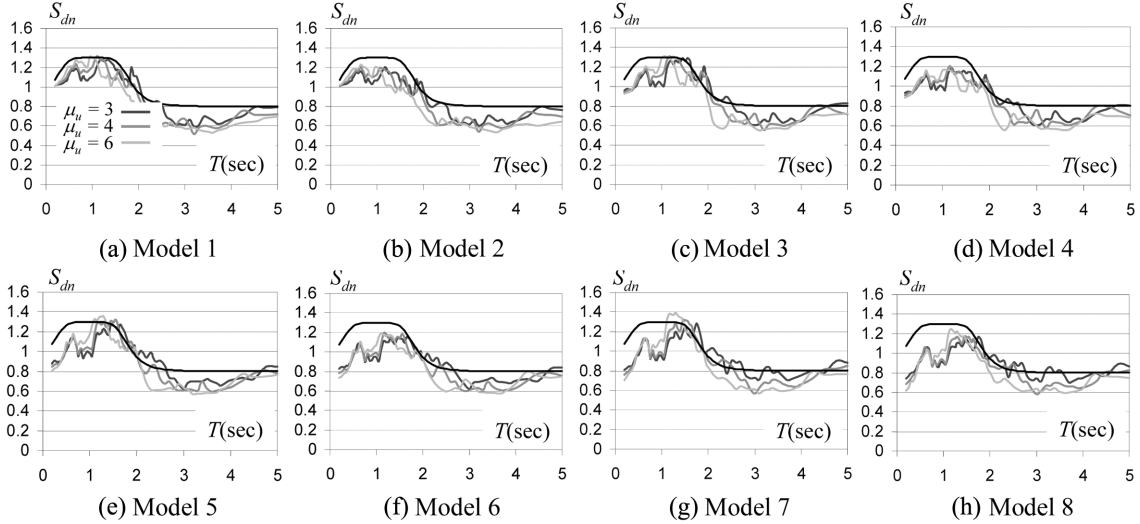


Fig. 4 Normalized displacement spectra for constant damage ( $DMI_{PA} = 1$ ), Lake Zone of Mexico City, 5% critical damping

where  $S_{dy}$  refers to displacement at yield. Note that the values of  $S_{an}$  and  $S_{dn}$  are similar only in the case in which the maximum ductilities corresponding to degrading and elasto-perfectly-plastic behaviors are similar. Fig. 4 shows mean normalized displacement spectra for constant damage ( $DMI_{PA} = 1$ ). The black curve corresponds to Eq. 5. Although Figs. 2 and 4 exhibit similar overall tendencies, for  $\beta$  equal or larger than 0.15 (models 5 to 8) the values of  $S_{dn}$  tend to be significantly smaller than those of  $S_{an}$  for periods less than one second ( $0.5 T_g$ ). The differences observed for  $S_{an}$  and  $S_{dn}$  for short periods can be explained because the maximum ductilities developed by degrading systems in this range of period tend to be significantly smaller than those developed by their non-degrading counterparts. Note that Eq. 5 can be used to correct the strength and displacement demands read from spectra derived from elasto-perfectly-plastic behavior provided the period of the system is equal or larger than  $0.5 T_g$ . For a period smaller than  $0.5 T_g$ , Eq. 5 yields conservative displacement demands for degrading behavior.

Finally, it should be mentioned that the influence of hysteretic degradation is determined by the acceptable level of structural damage. On one hand, for immediate operation, structures should remain elastic, so that hysteretic behavior does not affect their performance. On the other hand, for life safety, the shape of the hysteresis loops has the effect discussed in Figs. 2 to 4. It can be said that degrading behavior has an intermediate effect for intermediate limit states.

#### 4. Constant cumulative ductility spectra

A constant *cumulative* ductility strength spectrum corresponding to a *cumulative* ductility  $NE_{H\mu}$  is defined so that its ordinates evaluated at any value of  $T$  will result in a lateral strength that is capable of controlling the *cumulative* ductility demand on a SDOF system within the threshold value of  $NE_{H\mu}$  (Teran and Bahena 2007). As in the case of *maximum* ductility strength spectra, the ordinates of constant *cumulative* ductility strength spectra correspond to pseudo-acceleration ( $S_a$ ). In

the case of elasto-perfectly-plastic systems,  $NE_{H\mu}$  is actually equal to the *cumulative* plastic ductility demand. For systems exhibiting deterioration of their hysteretic behavior this notation is not strictly correct, but the concept is directly applicable to their seismic design. The use of *cumulative* ductility strength spectra within the context of the static method of analysis is similar to the current use of strength spectra:

- A. Determine the design values of  $T$  and  $NE_{H\mu}$  associated to the structure to be designed. The value of  $NE_{H\mu}$  can be established from Eq. 3 according to the ultimate and cumulative ductility capacities of the structure ( $\mu_u$  and  $b$ , respectively); and thus, according to the detailing to be used in the structure.
- B. Evaluate at  $T$  the constant *cumulative* ductility  $S_a$  spectrum corresponding to  $NE_{H\mu}$ .
- C. Provide the structure with a minimum base shear corresponding to  $S_a(T, NE_{H\mu}) W$ , where  $W$  is the total reactive weight of the structure.

Although the design of the lateral strength of a structure through the use of *cumulative* ductility strength spectra follows the same steps currently used for strength design, *cumulative* ductility strength spectra are targeted to control the *cumulative* plastic deformation demand in lieu of focusing, as traditional strength spectra do, on controlling the *maximum* plastic deformation demand. The use of *cumulative* ductility strength spectra requires the definition of strength reduction factors that take into consideration the effect of cumulative plastic deformation. Terán and Bahena (2007) have developed equations to estimate strength reduction factors for structures located in the Lake Zone of Mexico City. Because *cumulative* ductility spectra consider explicitly the effect of cumulative plastic deformation demands, it is possible to use them as a manner to correct the strength under-design resulting from the use of traditional design strength spectra.

## 5. Performance-based numerical seismic design

In recent decades, several researchers and practicing engineers have talked about performance-based design as a rational basis for the formulation of seismic design methodologies. The Vision 2000 Committee (SEAOC 1995), has proposed a global design process formed by three phases: Conceptual, Numerical, and Implementation. A numerical performance-based methodology requires that the response of the structural and non-structural members be checked against threshold levels established as a function of the required seismic performance. Recently proposed design methodologies contemplate this check at three different steps:

*Global Predesign.* Quick and reasonable estimates of global seismic demands should be established and checked against global threshold levels. Within this context, the judicious use of response spectra provides information that allows the determination of a set of global mechanical characteristics (base shear, period of vibration, damping coefficient, and ultimate deformation capacity) that can adequately control and accommodate, within technical and cost constraints, the global response of the structure.

*Preliminary Local Design.* Once the global mechanical characteristics have been determined, it is necessary to establish the structural properties and detailing at the local level. This step contemplates the analyses of complex analytical models of the structure, to obtain design information for the sizing, strength design and detailing of the structural elements.

*Revision of the Preliminary Design.* Some recommendations have been formulated for the revision of the preliminary design through a series of dynamic structural analyses that address the global and

local performance of the structure (e.g., Bertero and Bertero 1992, Federal Emergency Management Agency 1997).

Within the context of performance-based design, the structural properties should be provided in such way that, within technical and cost constraints, the structure is capable of controlling and accommodating adequately, for every relevant limit state, its dynamic response. The seismic design methodology introduced in this paper takes into consideration the *Global Predesign* and *Preliminary Local Design* steps. The methodology applies to the design of structures having standard occupancy, and considers the immediate operation and life safety limit states. It will be assumed that during the *Conceptual Phase*, the engineer has decided to use reinforced concrete ductile frames as the structural system of the building, and that the structural and non-structural performance should be addressed during the *Numerical Phase*.

### 5.1 Preliminary design

Within the context of performance-based seismic design, the solution given to the design problem has to be efficient and yield adequate performance. A deficient preliminary solution can easily result on a limited final design that is far from the optimal solution. Thus, the adequate conception and predesign of the structure become relevant to its seismic design.

Fig. 5 summarizes schematically the *Global Predesign* phase of the proposed methodology. The objective of *Global Predesign* is to establish at the global level the value of three mechanical characteristics of the structure. These characteristics, denoted herein design parameters, are related to the lateral strength, lateral stiffness and ultimate deformation capacity of the structure.

*Global Predesign* initiates with a qualitative definition of what is considered acceptable structural and non-structural performance. Note that acceptable performance is formulated in terms of threshold levels of damage associated to the limit states under consideration.

The ultimate deformation capacity of a ductile reinforced concrete frame can be characterized through values of ultimate ductility,  $\mu_u$ , ranging from 4 to 6. Note that this ductility is referred to the roof displacement, and is considered in Fig. 5 equal to 5. It should be mentioned that the  $\mu_u$  measured during experimental tests of ductile reinforced concrete elements and sub-assemblages have reached values of 8 and larger. In this respect, the range of values of  $\mu_u$  indicated before is considered a reasonable lower bound for design purposes.

The next step in *Global Predesign* implies the quantification of acceptable performance by establishing thresholds to the global response of the structure with the aid of damage indices. Finally, the value of the other two design parameters (the fundamental period of vibration that quantifies the design requirements of lateral stiffness, and the base shear that quantifies the design lateral strength) is established with the aid of displacement and strength spectra. Once the value of the three design parameters is established, the methodology proposed herein proceeds to the *Preliminary Local Design* (local design of strength, stiffness and deformation capacity).

In the case of immediate operation: A) Although some possible loss of stiffness due to cracking is considered acceptable, the structural elements of the frame should not exhibit a loss in their lateral strength and ultimate deformation capacity; B) The non-structural system should remain undamaged. It is considered that the structural elements satisfy their performance conditions if they remain elastic, and that damage to non-structural elements can be avoided if the maximum interstory drift index demand ( $IDIO$ ) is controlled within the threshold of 0.004.

The building should guarantee the physical integrity of its occupants for life safety, in such

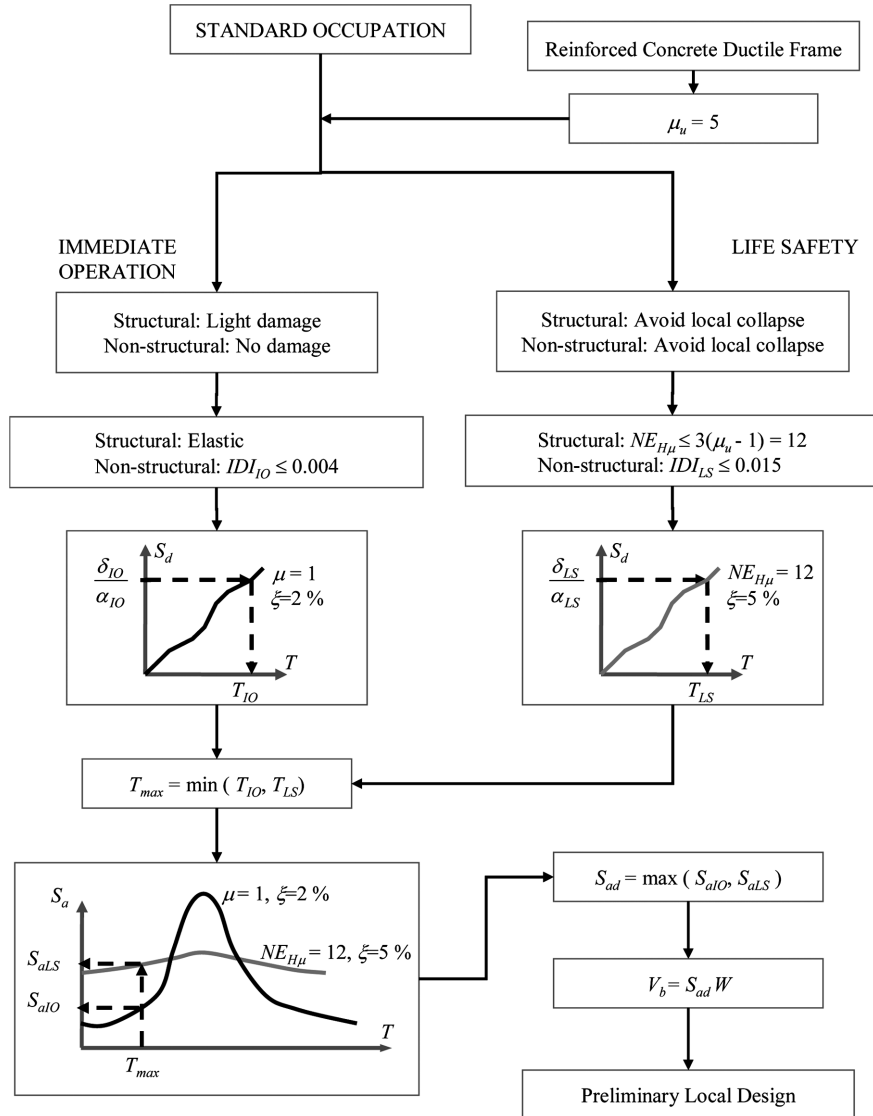


Fig. 5 Global Predesign

manner that local and global collapse should be prevented. According to the methodology introduced herein, this implies: A) Limiting structural damage through establishing a normalized energy threshold according to the Teran and Jirsa damage index [ $NE_{H\mu} = 3(\mu_u - 1) = 12$ ]; and B) Limit non-structural damage through controlling the maximum interstory drift index demand ( $IDI_{LS}$ ) within the threshold of 0.015. It should be noted that the threshold values for  $IDI_{IO}$  and  $IDI_{LS}$  should be established as a function of the non-structural elements and of the detailing used on their connection to the structural system. The proposed methodology can and should explicitly consider different drift thresholds according to the characteristics of the non-structural system.

The value of the fundamental period of vibration of the building is established according to Fig. 5. The interstory drift index threshold for a given limit state can be used to establish the lateral roof

displacement threshold for that limit state

$$\delta_{IO} = \frac{IDI_{IO}H}{COD_{IO}} \quad (9a)$$

$$\delta_{LS} = \frac{IDI_{LS}H}{COD_{LS}} \quad (9b)$$

where  $H$  is the total height of the building, and  $COD$  a coefficient of distortion that contemplates that interstory drift is not constant throughout the height of the building. Particularly,  $COD$  quantifies the ratio of the maximum interstory drift index to the average interstory drift index (Qi and Moehle 1991). Table 1 summarizes values of  $COD$  for predesign of fairly regular frames.

The fundamental period of vibration of the building can be estimated through the use of the displacement thresholds  $\delta_{IO}$  and  $\delta_{LS}$  and displacement spectra corresponding to both limit states. For this purpose,  $\delta_{IO}$  and  $\delta_{LS}$  should be modified to take into consideration multi-degree-of-freedom effects. According to what is shown in Fig. 5, the roof displacement threshold should be corrected through the use of parameter  $\alpha$ . Based on the recommendations of FEMA 306 (Applied Technology Council 1998) and Teran (2004), Table 2 presents values of  $\alpha$  for predesign of frames.

According to the acceptable level of damage for each limit state, the displacement spectrum for immediate operation contemplates elastic behavior and a percentage of critical damping ( $\xi$ ) equal to 2%. In the case of life safety, the spectrum corresponds to  $NE_{H\mu} = 3(\mu_u - 1) = 12$  and  $\xi$  of 5%.

Fig. 5 indicates that the design value for the fundamental period of vibration ( $T_{max}$ ) is equal to the smaller of the values that satisfy the design requirements imposed by both limit states. The experimental evidence cited by Reyes (2000) suggests that a ductile reinforced concrete frame exhibits incipient yielding at interstory drift index demands close to 0.005, in such manner that considerably cracking is expected on it for interstory drifts close to the threshold considered for immediate operation ( $IDI_{IO} = 0.004$ ). Under these circumstances, the elastic lateral stiffness for both limit states under consideration is similar, and the sizing of the structural elements is defined by the smaller of  $T_{IO}$  and  $T_{LS}$ . Under certain circumstances, the smaller of  $T_{IO}$  and  $T_{LS}$  won't represent the

Table 1 Range of values of  $COD$

Global Ductility	$COD$	
	Minimum	Maximum
1	1.2	1.5
2+	1.5	2.0

Table 2 Values of  $\alpha$

Stories	$\alpha$	
	$\mu = 1$	$\mu = 2+$
1	1.0	1.0
2	1.2	1.1
3	1.3	1.2
5+	1.4	1.2

critical condition. For example, consider the case in which immediate operation is associated to a smaller interstory drift index threshold, in such manner that little cracking is expected in the structural elements. Because the elastic lateral stiffness for immediate operation would be considerably larger than that corresponding to life safety, it could happen that the critical condition for the sizing of the structural elements arises from life safety in spite that  $T_{LS}$  is larger than  $T_{IO}$  (Bertero and Bertero 1992).

The value of the design base shear ( $V_{bd}$ ) is estimated as the larger of the base shears established for both limit states. While for immediate operation the base shear is established from an elastic strength spectrum corresponding to  $\xi$  of 0.02; the spectrum corresponding to life safety is defined for  $NE_{Hu} = 12$  and  $\xi$  of 0.05. If the structure is analyzed using the static method of analysis, the lateral forces can be directly derived from  $V_{bd}$ . If required, modal spectral analysis could be carried out using the spectra corresponding to both limit states, and the strength demands on the structural elements of the frame derived from the critical condition.

Once the value of the three design parameters is established ( $\mu_u$ ,  $T_{max}$  and  $V_{bd}$ ), the design proceeds to *Preliminary Local Design*. The details involved in this step will be discussed as the example of application is developed.

## 5.2 Design seismic excitations

Two sets of ground motions recorded in the Lake Zone of Mexico City were used to establish design spectra. The first set, corresponding to immediate operation, included the motions summarized in Table 3, scaled so that their peak ground velocity matched one fourth of the peak ground velocity of the motion recorded during 1985 in the east-west direction of the *Secretaria de Comunicaciones y Transportes* (SCTEW). The second set, corresponding to life safety, is summarized in Table 4. The motions included in the second set were scaled so that their peak ground velocity matched that of the SCTEW motion. The design elastic strength spectrum for each set was determined from the mean plus one standard deviation of the corresponding spectra derived from each motion within that set. In the tables,  $T_g$  denotes the dominant period of motion. In the

Table 3 Ground motions considered for Immediate Operation

Id	Location	Date	$PGA^1$ (cm/sec <sup>2</sup> )	$PGV^2$ (cm/sec)	$T_g$ (sec)
s43	Garibaldi EW	10/12/94	13.9	5.38	2.1
s45	Garibaldi EW	14/09/95	30.5	9.73	2.0
s46	Garibaldi NS	14/09/95	26.0	8.04	2.1
s59	Liverpool EW	09/10/95	16.5	6.19	2.1
s77	Tlatelolco EW	10/12/94	14.9	4.58	2.1
s79	Tlatelolco EW	14/09/95	26.7	7.91	2.0
s89	Alameda EW	14/09/95	40.6	10.54	2.0
s119	C.U Juarez EW	10/12/94	14.8	4.47	1.9
s129	Cibeles EW	09/10/95	14.3	5.11	2.0
s131	Angares EW	14/09/95	29.6	9.50	1.6
s143	Tlatelolco NS	14/09/95	19.1	8.38	1.9
s140	SCT EW	25/04/89	40.0	19.45	2.0

<sup>1</sup> Original Peak Ground Acceleration

<sup>2</sup> Original Peak Ground Velocity

Table 4 Ground motions considered for Life Safety

Id	Location	Date	$PGA^1$ (cm/sec <sup>2</sup> )	$PGV^2$ (cm/sec)	$T_g$ (sec)
mx01	Alameda EW	04/25/89	45.83	15.103	2.1
mx03	Garibaldi EW	04/25/89	52.24	17.484	2.2
mx04	Tlahuac EW	09/19/85	117.63	34.575	2.1
mx06	Tlahuac NS	09/21/85	49.26	13.108	2.0
mx07	Tlahuac EW	09/21/85	51.47	15.098	1.9
mx08	SCT EW	09/19/85	167.26	61.074	2.0

case of the life safety limit state, the constant *cumulative* ductility strength spectrum used for design was established by reducing the mean +  $\sigma$  elastic strength spectrum by the reduction factors proposed by Teran-Gilmore and Bahena-Arredondo (2008) for elasto-perfectly-plastic behavior. Because currently there is a lack of expressions to establish *cumulative* ductility displacement spectra from an elastic displacement spectrum, the *cumulative* ductility displacement spectra used for design were established directly from the mean +  $\sigma$  spectra obtained from the motions included in Table 4 and elasto-perfectly-plastic behavior. Because both the design strength and displacement spectra for life safety corresponded to elasto-perfectly-plastic behavior, the ordinates of both spectra were modified by Eq. 5 to take into account the degradation of the hysteretic cycle.

## 6. Example of application

Fig. 6 shows plan and elevation views of the reinforced concrete building under consideration. The building has 12 stories, and regular distributions of mass, strength and stiffness in plan and height. While the height of the ground story is 5 meters, the rest of the stories have a height of 4 meters. The building has, in each of its two principal directions, three bays with a length of 7

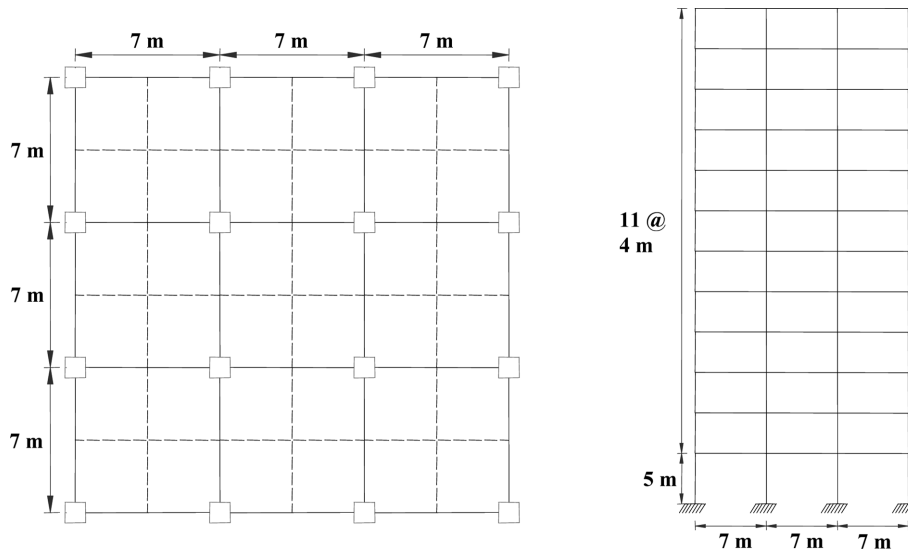


Fig. 6 Plan and elevation views of the building

meters. For simplification purposes, the same sizes and reinforcement were used for the structural elements of the four frames aligned in each principal direction. The nominal strength of the structural materials are  $f'_c$  of 350 kg/cm<sup>2</sup> for concrete and  $f_y$  of 4200 kg/cm<sup>2</sup> for reinforcing steel.

### 6.1 Global Predesign

As shown in Fig. 5, the value of 5 is considered representative of the  $\mu_u$  of reinforced concrete frames. Regarding the values of  $COD$  used, it should be considered that the value of this parameter increases with increments in the number of stories and of the plastic deformation demand in the building, and for larger stiffness and strength irregularities through height. Considering the regularity and height of the building, it was decided to assign to the building values of  $COD$  that are close to the lower bounds offered in Table 1

$$\delta_{IO} = \frac{IDI_{IO}H}{COD_{IO}} = \frac{0.004 \times 49}{1.2} = 0.163 \text{ m} = 16.3 \text{ cm} \quad (10a)$$

$$\delta_{LS} = \frac{IDI_{LS}H}{COD_{LS}} = \frac{0.015 \times 49}{1.6} = 0.459 \text{ m} = 46 \text{ cm} \quad (10b)$$

Before using displacement spectra to estimate the fundamental period of vibration of the building, the roof displacement need to be corrected through the  $\alpha$  factor summarized in Table 2

$$S_{dIO} = \frac{16.3}{1.4} = 11.66 \text{ cm} \quad (11a)$$

$$S_{dLS} = \frac{46}{1.2} = 38.33 \text{ cm} \quad (11b)$$

The period for which the structural elements of the frame should be sized corresponds to the smaller of those derived from Fig. 7. This results in  $T_{max} = 1.25$  seconds. The stiffness-based sizing of the frames should be carried out in such manner that the fundamental period of vibration of the building is equal or slightly less than  $T_{max}$ . A possibility is to establish an analytical model of the

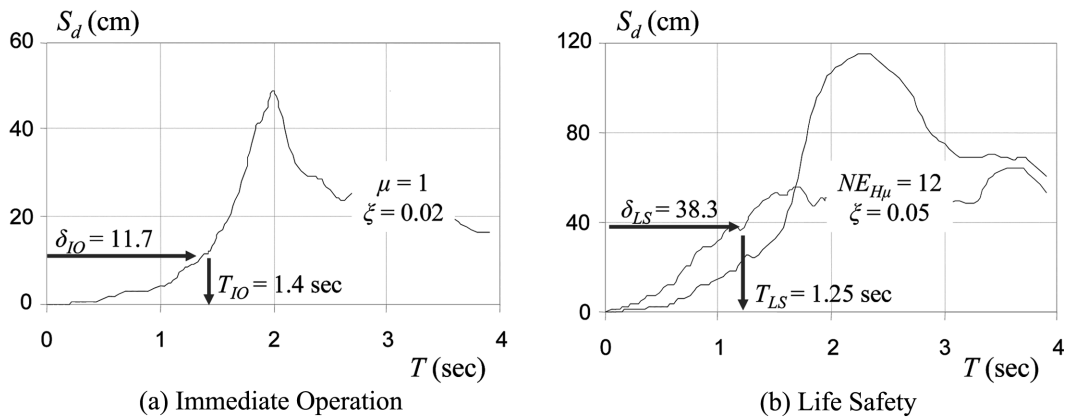


Fig. 7 Determination of the fundamental operation period of vibration of the building

building, and iterate with the area of the structural elements until getting the desired period.

Once the value of  $T_{max}$  is available, it is possible to define which one of the two strength spectra shown in Fig. 8 should be used for a modal spectral analysis of the structure. Because of its larger ordinates in the range of periods of interest, the dynamic analysis should be carried out using the life safety design strength spectrum.

It is important to note that both design strength spectra have been reduced to account for the expected overstrength in the building. In the case of life safety, the overstrength factor ( $R$ ) is defined as the ultimate lateral strength normalized by the design lateral strength. Miranda (1991) proposed the following expression to estimate the lateral overstrength

$$R = 2 - 0.5 \sqrt{\frac{T}{5}} \quad (12)$$

For a 12-story building, the fundamental period of vibration should be close to 1.2 sec, in such manner that according to Eq. 12,  $R$  should be close to 1.75. Other studies suggest that the lateral overstrength for ductile frames located in the Lake Zone of Mexico City and designed according to the Mexico City Building Code is close to two (Teran 1998). According to this,  $R$  should oscillate between 1.75 and 2.0.

Recently, Teran (2004) observed that seismic design that accounts for cumulative deformation demands requires that the base shear of the structure is close to that estimated according to the static method of analysis; that is, even if a dynamic analysis is carried out, the design base shear should not be less than the static base shear. Considering that in the Lake Zone of Mexico City the dynamic response of a building is dominated by the fundamental mode of vibration, the dynamic base shear is usually close to 80% of the static base shear. Under these circumstances, the dynamic analysis will only result in a base shear that is close to the static base shear if the overstrength factor used to reduce the design spectra is equal to  $0.8R$ . The overstrength factor to be used during the dynamic analysis can be estimated then as  $0.8R = 0.8 (1.75 \text{ to } 2.0) = 1.4 \text{ to } 1.6$ . In this paper,  $R = 1.5$  was used to reduce the life safety strength spectra to carry out the dynamic analysis of the building (the ordinates in Fig. 8(b) are already divided by 1.5).

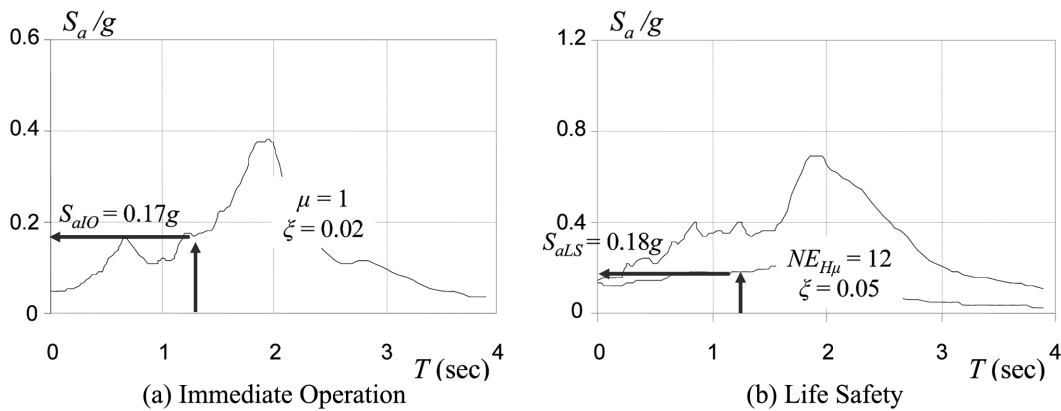


Fig. 8 Determination of the base shear of the building

Regarding immediate operation, the lateral overstrength is associated to the lateral yield strength rather than to the ultimate lateral strength. This implies that the value of  $R$  associated to immediate operation should be greater than one, and less than the value of  $R$  used for life safety. It was decided to reduce the design strength spectra for immediate operation by a factor of 1.2 (the ordinates in Fig. 8(a) are already reduced by this factor).

As a reference, the total reactive weight of the 12-story building is 6200 tons. Taking into consideration that life safety is the critical condition for strength design, the required static base shear in the building according to Fig. 8(b) is  $V_{bST} = 0.18 \times 1.5 \times 6200 = 1680$  tons, which implies that each one of the four frames should be able to develop a base shear of 420 tons.

Once the global mechanical characteristics of the building are established ( $\mu_u = 5$ ,  $T_{max} = 1.25$  sec and  $V_{bd} = 1680$  tons) the methodology proceeds to the local preliminary design. Note that: A) Life safety rules the stiffness and strength design of the building; and B) The value estimated for the design base shear is only a reference; a modal spectral analysis of the building will be carried out using the design spectrum shown in Fig. 8(b).

## 6.2 Preliminary Local Design

The *Preliminary Local Design* initiates with the sizing of the structural elements. For this purpose, a series of eigenvalue analyses are carried out until the sizes of beams and columns are such that the fundamental period of vibration of the building is equal or slightly smaller than  $T_{max}$ . The moment of inertia of a beam was estimated as the average of its positive and negative moments of inertia (the positive moment of inertia was estimated from a “T” section that considers the slab width in compression specified by the ACI code, and the negative one from a rectangular section). The structural elements were considered cracked, and based on the recommendations given by FEMA 273, their moment of inertia was assumed to be  $0.5 I_g$  and  $0.7 I_g$  for beams and columns, respectively ( $I_g$  is the gross section moment of inertia). The sizes summarized in Table 5 results in a fundamental period of vibration for the building of 1.24 sec.

Once the preliminary sizing is carried out, the local strength design can be carried out through the use of static or dynamic methods of analysis. In the case of this paper, the design lateral forces were derived from a modal spectral analysis that used the design strength spectrum shown in Fig. 8(b). The beams were designed according to the Complementary Technical Requirements for the Design and Construction of Reinforced Concrete Structures of the Mexico City Building Code. Table 5 summarizes the negative and positive (between parenthesis) longitudinal steel at the beams’ ends.

Table 5 Sizes of structural elements

Story	Beams			Columns		
	Sizes (cm)	Type 1	Type 2	Sizes (cm)	External	Internal
1, 2 and 3	50 x 120	7#10 (5#10)	6#10 (4#10)	90 x 90	32#8	36#10
4, 5 and 6	40 x 120	6#10 (5#8)	5#10 (6#8)	90 x 90	16#8	20#10
7, 8 and 9	40 x 110	5#10 (5#8)	5#10 (5#8)	90 x 90	16#8	20#8
10, 11 and 12	40 x 100	5#8 (3#8)	5#8 (3#8)	90 x 90	16#8	20#8

Once the beams were designed, capacity design concepts were applied to obtain the longitudinal steel of the columns summarized in Table 5. Several columns exhibit the same amount of longitudinal steel because of the minimum steel requirements indicated in the code.

The third step during local preliminary design is the detailing of the structural elements. This step was carried out according to the requirements indicated in the Complementary Technical Requirements for the Design and Construction of Reinforced Concrete Structures for ductile frames (which are very similar to the ACI requirements for special moment-resisting frames).

## 7. Mechanical characteristics of the 12-story building

A two dimensional, lumped plasticity nonlinear model of one of the central frames of the 12-story building was established. An attempt was made to capture in a reasonable manner the strength, stiffness and deformation capacity of its structural members. The strength capacity of the reinforced concrete members was calculated using expected strength values of the structural materials. Particularly, the expected strength of Mexican reinforcement bars was established according to the studies carried out by Rodriguez and Botero (1997). Regarding the flexural stiffness, the expected level of cracking on beams and columns was taken explicitly into consideration. The local deformation capacity of the structural members was characterized through the ultimate plastic rotation capacity that their ends (plastic hinges) could accommodate. Finally, the effect that the slab has on the structural properties of the beams was also considered.

In summary, well known analytical models for stress-strain curves of confined and unconfined concrete, as well as for steel, were adopted. With the properties and considerations discussed in the previous paragraph, moment-curvature curves for the cross-sections at both ends of the reinforced concrete structural members were established. For this purpose, it was assumed that a plane section remains plane after deformation. Bilinear idealizations of these curves were established by defining yield and ultimate curvatures. The yielding moment of a section,  $M_y$ , and its corresponding curvature,  $\phi_y$ , were defined as the moment and curvature at which any longitudinal bar in a section reaches first yielding. The ultimate curvature,  $\phi_u$ , was defined as the smaller of the curvatures corresponding to the following two conditions: A) The concrete in the section reaches its maximum compressive strain (it crushes), or B) One of the longitudinal bars in tension reaches its ultimate strain (it fractures). The ultimate flexural moment in a section,  $M_u$ , was defined as the flexural moment the section exhibits when it reaches its ultimate curvature. By connecting the origin to the point defined by  $(M_y, \phi_y)$  through a straight line, and connecting the latter point to the point defined by  $(M_u, \phi_u)$  through another straight line, the bilinear moment-curvature diagram of the section was defined.

The strength, stiffness and deformation capacity of the structural members were then established directly from these bilinear curves. Particularly, the strength of each section is characterized by its flexural capacity at yield ( $M_y$ ). In the case of the beams, two flexural capacities were defined, one for positive bending (T section) and one for negative bending (rectangular section). In the case of the columns, the *axial force-flexural moment* interaction was explicitly considered. While the “cracked section” flexural stiffness of the sections were estimated directly from the slope corresponding to the elastic part of the bilinear diagram, their strain hardening was established from the slope corresponding to the plastic region of the diagram. The flexural stiffness at one end of a beam was estimated as the average value of the positive and negative stiffnesses at that end. The flexural

stiffness of the entire beam was computed as the average of the stiffnesses corresponding to its two ends. Finally, the ultimate deformation capacity at the ends of the structural members was characterized by

$$\theta_u = (\varphi_u - \varphi_y)L_p \tag{13}$$

where  $\theta_u$  is the ultimate plastic rotation capacity of the section, and  $L_p$  the plastic hinge length (assumed equal to half the effective height of the beam).

The portion of slab that interacted, in tension as well as in compression, with the beams was defined according to the recommendations of Pantazopoulou and French (2001) for a 2% interstory drift. Because of limitations inherent to *DRAIN 2DX* (Prakash *et al.* 1993), program used to carry out the non-linear analyses, the stiffness of the structural elements was assumed to be independent of their level of axial force. The columns in the first story were modeled as clamped at their bases. Strain hardening and second order effects were explicitly considered.

A pushover analysis of the building was carried out by using a lateral force distribution through height that remained proportional to that derived from the modal spectral analysis. Fig. 9(a) shows the base shear versus roof displacement curve for the building. According to *DRAIN 2DX*, the frame

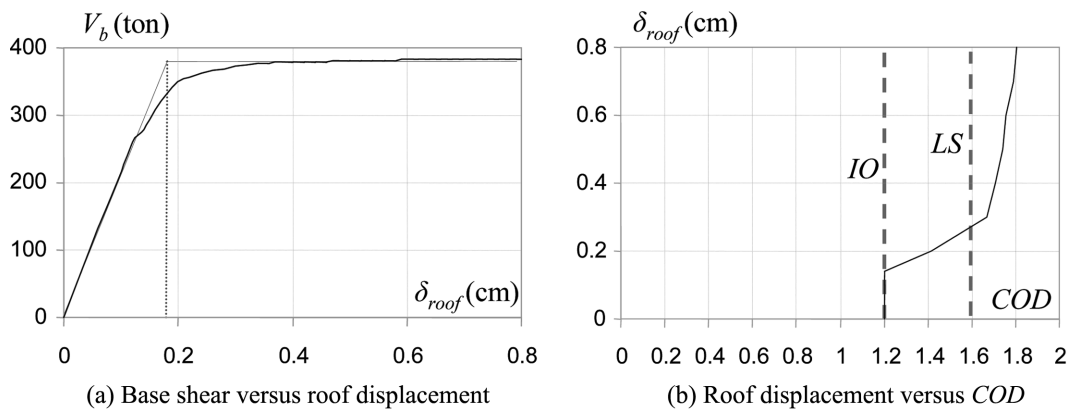


Fig. 9 Results derived from static non-linear analysis of 12-story building

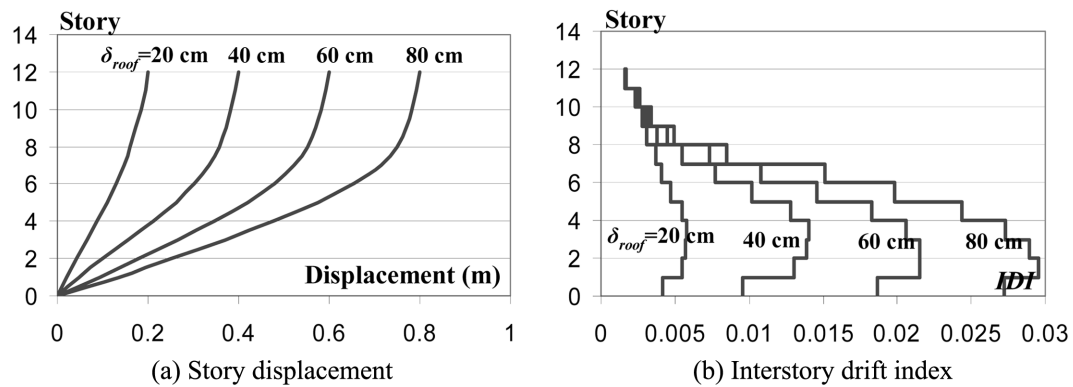


Fig. 10 Evolution of lateral deformation distribution through height

is capable of developing an ultimate base shear of 390 tons. As discussed before, the design base shear is equal to 420 tons per frame, in such manner that there is a small under-design of lateral strength. The frame is able to develop an ultimate global ductility of  $\mu_u = \delta_u / \delta_y = 0.80 / 0.17 = 4.7$  ( $\delta_u$  is the ultimate roof displacement and  $\delta_y$  the roof displacement at yield derived from a bilinear idealization of the base shear versus roof displacement curve).  $\delta_u$  was defined as that in which the rotational capacity of at least one third of the beams in the critical story is exhausted. The value of 4.7 is similar to the value of 5 considered during the global predesign of the frame. Fig. 9(b) shows the evolution of the *COD* of the frame as a function of an increasing roof displacement ( $\delta_{roof}$ ). It can be concluded that the values of *COD* used during global predesign (indicated in discontinuous lines) are congruent with those actually estimated for the building.

Although not shown, the frame develops a weak-beam/strong-column mechanism. Fig. 10 shows the distributions of lateral displacement and interstory drift index through height for roof displacements of 20, 40, 60 and 80 cm. The interstory drift index distribution corresponding to yield (roof displacement of 20 cm) shows a fairly uniform distribution of lateral deformation through height, with maximum values close to 0.005. This is congruent with the experimental evidence gathered by Reyes (2000), which suggests that ductile reinforced concrete frames yield at interstory drift indices close to 0.005.

The height distribution of lateral deformation changes with an increase in roof displacement. Particularly, as the plastic demands increase in the building, the lower stories accumulate larger lateral deformation with respect to the other stories. For the roof displacement at ultimate (80 cm), the lower stories reach an interstory drift index close to 0.03, value that is congruent with the threshold of 0.04 indicated by Reyes (2000) as the ultimate interstory capacity of ductile reinforced concrete frames.

Figs. 9 and 10 reflect the design objectives in the mechanical characteristics of the building. Regarding immediate operation, the design objective requires the structural elements to remain elastic while adequate non-structural performance is promoted through controlling the maximum interstory drift index within the threshold of 0.004 (Fig. 5). According to Fig. 9(a), the idealized roof yield displacement of the building is 18 cm, in such manner that controlling the roof displacement within the threshold of 16.3 cm (see Eq. 10(a)) results in that the structural elements remain elastic. According to Fig. 10(b), the maximum interstory drift index for a roof displacement of 20 cm is about 0.0055. Considering that the maximum interstory drift index for a roof displacement of 16.3 cm is proportional to that corresponding to 20 cm,  $IDI_{IO} = (0.0055)16.3/20 = 0.0045$ , value that is congruent with the threshold of 0.004 contemplated in Fig. 5.

Regarding life safety, the design objective requires that the cumulative plastic deformation demands be controlled so as to avoid local collapse. For a structure subjected to large energy demands, this implies controlling its global ductility demand to a value close to 50% of its ultimate ductility (Bertero 1997, Panagiotakos and Fardis 2001). In the case of the 12-story building, 50% of its ultimate deformation capacity is equal to 40 cm, value that is very similar to the threshold of 46 cm established with Eq. 10(b). According to Fig. 5, adequate non-structural performance is promoted through controlling the maximum interstory drift index demand within the threshold of 0.015. According to Fig. 10(b), the maximum interstory drift index for a roof displacement of 40 cm is close to 0.0135. Under the assumption of proportionality, the drift demand for a roof displacement of 46 cm can be estimated as  $IDI_{LS} = (0.0135)46/40 = 0.0155$ , value that is congruent with the design threshold of 0.015. It can be concluded that for life safety, non-structural performance and the cumulative plastic deformation demands result in that the building should

Table 6 Mechanical characteristics of 12-story building

Characteristic	Design parameter	D2DX Non-linear model
Stiffness	$T_{max} = 1.25$ sec	$T_{max} = 1.3$ sec
Strength	$V_b = 420$ ton per frame	$V_b = 390$ ton per frame
Deformation capacity	$\mu_u = 5$	$\mu_u = 4.7$
Mechanism	Weak beam- strong column	Weak beam- strong column

control its maximum roof displacement within the threshold of 46 cm, and thus, that it can not develop during the design ground motion its full ultimate deformation capacity of 80 cm.

According to the results summarized in Table 6, the mechanical characteristics of the 12-story frame closely reflect the values of the design parameters obtained during global predesign.

## 8. Seismic performance of 12-story building

The seismic performance of the building was estimated for immediate operation and life safety through non-linear time-history analyses. Because extensive cracking is expected on the structural elements for both limit states, the same non-linear model is used for them. If the expected level of cracking is different, then it would be necessary to establish two different models. For the non-linear dynamic analyses, the pushover model was adapted in such manner that viscous damping was considered through a Rayleigh matrix. The first two modes of the frame were assigned 2% and 5% critical damping for immediate operation and life safety, respectively.

On one hand, it should be mentioned that the larger approximation made by using the same nonlinear model for both limit states is that the slab width contributing to the structural properties of the beams depends on the level of interstory drift index, in such manner that the width corresponding to immediate operation is less than that for life safety. For life safety, the interstory drift index demands are congruent with those considered by Pantazopoulou and French (2001). On the other hand, the beams of the 12-story building are fairly robust and exhibit large steel content, in such manner that the contribution of the slab to the structural properties of the beams is not significant.

### 8.1 Immediate Operation

While an interstory drift index threshold of 0.004 was established to formulate non-structural damage control, structural damage control was formulated through keeping the structural elements within their elastic range of behavior. To evaluate the seismic performance of the 12-story building, the *DRAIN 2DX* model was subjected to the ground motions included in Table 3. Fig. 11(a) shows the maximum interstory drift index demands for each ground motion, and compares the mean + one standard deviation ( $\sigma$ ) demand with the design threshold. The number assigned to each diamond corresponds to the story level at which the maximum demand was registered. The maximum interstory drift index for every ground motion is less than the design threshold, and thus, the mean +  $\sigma$  demand, which is close to 0.003, does not exceed that threshold. According to this, the non-structural performance of the frame satisfies the requirements imposed by the design objectives. Regarding the structural performance, the structural elements remained elastic during all the ground motions under consideration.

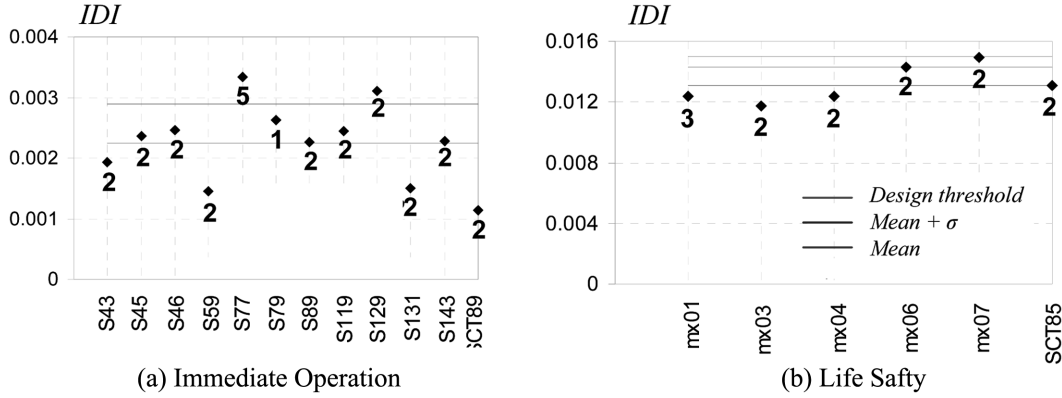


Fig. 11 Evaluation of non-structural performance

### 8.2 Life Safety

While an interstory drift index threshold of 0.015 was established to formulate non-structural damage control, structural damage control was formulated through controlling the local plastic deformation demands in such manner that local collapse is avoided. To evaluate the seismic performance of the 12-story building, the *DRAIN 2DX* model was subjected to the ground motions included in Table 4. For this purpose, a modified version of the *DRAIN 2DX* program, capable of modeling the degradation of the reinforced concrete elements through the Takeda model, was used (Ascheim 2005). Fig. 11(b) shows the maximum interstory drift index demand for each ground motion, and compares the mean + $\sigma$  demand with the design threshold. Because all interstory drift index demands are smaller than the design threshold, the mean + $\sigma$  demand does not exceed the design threshold. It can be concluded that non-structural performance of the frame satisfies the design requirements imposed by the design objectives.

Local structural damage (at the element level) was evaluated at the ends of the beams, where the plastic deformation demands tend to accumulate. Damage was estimated with a modified version of the Park and Ang damage index

$$DMI_{PA} = \max\left(\frac{\phi_{max}^+}{\phi_u^+}, \frac{\phi_{max}^-}{\phi_u^-}\right) + \beta\left(\frac{E_H^+}{M_y \phi_u^+} + \frac{E_H^-}{M_y \phi_u^-}\right) \quad (14)$$

where  $\phi_u$  is the ultimate curvature capacity,  $\phi_{max}$  is the maximum curvature demanded by the ground motion,  $E_H$  is the plastic energy dissipated in the plastic hinge, and  $M_y$  is the moment at yield. A positive sign implies positive bending; a negative one, negative bending.  $\beta$  of 0.15 was used, value that characterizes the stability of the hysteretic cycle of elements with seismic detailing. The experimental results obtained by Silva and Lopez (2001) suggest that Eq. 14 yields reasonable estimates of damage for reinforced concrete frames. While the value of  $DMI_{PA}$  for a beam is established from the largest value of  $DMI_{PA}$  estimated at both of its ends, the value of  $DMI_{PA}$  assigned to a story is obtained by averaging  $DMI_{PA}$  for all the beams located at that story.

Fig. 12 shows the mean + $\sigma$  structural damage distribution through height. Note that the largest damage tends to appear in the lower levels of the building, particularly in the second story. While

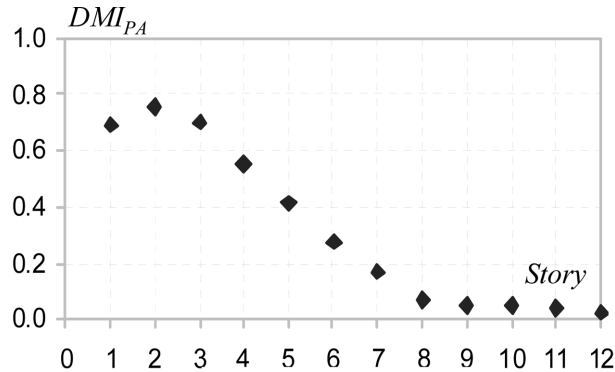


Fig. 12 Evaluation of structural damage, life safety

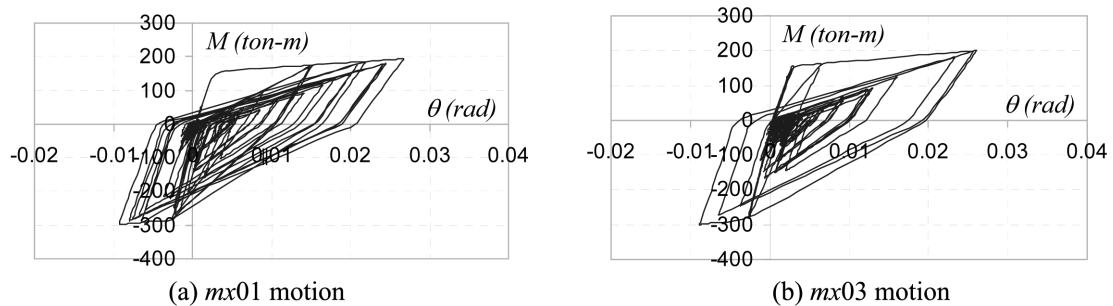


Fig. 13 Local response of critical beam during two ground motions

the mean damage index in the critical story is equal to 0.62, the mean  $+\sigma$  value exhibits a value close to 0.8. Because the latter value is smaller than the design threshold of one, it can be considered that the frame satisfies adequately the structural performance requirements imposed by the design objectives.

The evaluation of the structural performance of the frame indicates that the structural elements with the largest degree of damage are the beams located at the second level. Fig. 13 shows, for the *mx01* and *mx03* ground motions (Table 4), the hysteresis loops for the most damaged end of the critical beam of the frame. The hysteresis loops clearly reflect the stiffness degradation of the reinforced concrete beam. Taking into account that the plastic rotational capacity of the beams for positive and negative bending are close to 0.065 and 0.020, respectively, the end result of the application of the design methodology was to limit the rotation demands in the critical beams within thresholds that are about half of their ultimate deformation capacity.

## 9. Conclusions

The design strength spectra defined by current seismic design codes do not contemplate several variables that are relevant to the seismic performance of ductile reinforced concrete structures subjected to ground motions exhibiting large energy content. Among them, the following can be mentioned: 1) The cumulative plastic deformation demands; and 2) The effect of degradation of the

hysteretic cycle. Because the available experimental, analytical and field evidence suggest that this situation can result in a significant under-design of the lateral strength of reinforced concrete structures located in soft soils, it is necessary to study in more detail the effect of such variables, and to discuss carefully the convenience of increasing the design seismic coefficients corresponding to this type of soils.

An option to correct the possible lateral strength under-design of ductile structures is the concept of cumulative ductility spectra. In case of reinforced concrete structures, the ordinates derived from elasto-perfectly-plastic behavior should be modified to take into consideration the effect of the degradation of the hysteresis loops in the seismic demands.

The methodology proposed herein has been applied successfully to the design of a 12-story reinforced-concrete building located in the Lake Zone of Mexico City. The seismic performance of the building reflects adequately the behavior requirements imposed by the design objectives. A methodology such as the one introduced here can be used as a basis to incorporate performance-based concepts into the Mexico City Code. The results discussed herein create expectative for current codes to result in better seismic design through relatively small changes in their format.

## Acknowledgements

The authors gratefully acknowledge the economical support of Universidad Autonoma Metropolitana and the Consejo Nacional de Ciencia y Tecnologia.

## References

- Applied Technology Council (1998), "FEMA 306. Evaluation of earthquake damaged concrete and masonry wall buildings", ATC-43 Project.
- Ascheim, M (2005), <http://nisee.berkeley.edu/software/drain2dx>
- Arroyo, D. and Ordaz, M. (2007), "Hysteretic energy demands for SDOF systems subjected to narrow band earthquake ground motions. Applications to the Lake Bed Zone of Mexico City", *J. Earthq. Eng.*, **11**, 147-165.
- Bertero, R.D., and Bertero, V.V. (1992), "Tall reinforced concrete buildings: conceptual earthquake-resistant design methodology", Report UCB/EERC-92/16, University of California at Berkeley.
- Bertero, V.V. (1997), "Performance-based seismic engineering: A critical review of proposed guidelines", *Proceedings of the International Workshop on Seismic Design Methodologies for the Next Generation of Codes*, Rotterdam.
- Bojorquez, E. and Ruiz, S.E. (2004), "Strength reduction factors for the valley of Mexico taking into account low cycle fatigue effects", *Proceedings of the 13th World Conference on Earthquake Engineering*, Vancouver, August.
- Cosenza, E., Manfredi, G. and Ramasco, R. (1993), "The use of damage functionals in earthquake engineering: a comparison between different methods", *Earthq. Eng. Struct. D.*, **22**, 855-868.
- Fajfar, P. (1992), "Equivalent ductility factors taking into account low-cycle fatigue", *Earthq. Eng. Struct. D.*, **21**, 837-848.
- Federal Emergency Management Agency (1997), "FEMA 273, NEHRP guidelines for the seismic rehabilitation of buildings".
- Huerta-Garnica, B. and Reinoso-Angulo, E. (2002), "Espectros de energía de movimientos fuertes registrados en México", *Revista de Ingeniería Sísmica*, **66**, 45-72.
- Kunnath, S.K., Reinhorn, A.M. and Park, Y.J. (1990), "Analytical modeling of inelastic seismic response of R/C

- structures”, *J. Struct. Eng-ASCE*, **116**(4), 996-1017.
- Mahin, S.A. and Bertero, V.V. (1981), “An evaluation of inelastic seismic design spectra”, *J. Struct. Eng-ASCE*, **107**(9), 1777-1795.
- Miranda, E. (1991), *Seismic evaluation and upgrading of existing buildings*, Doctoral Thesis, University of California at Berkeley.
- Miranda, E. and Ruiz-García, J. (2002), “Influence of stiffness degradation on strength demands of structures built on soft soil sites”, *Eng. Struct.*, **24**(10), 1271-1281.
- Panagiotakos, T.B. and Fardis, M.N. (2001), “Deformations of reinforced concrete members at yielding and ultimate”, *ACI Struct. J.*, **98**(2), 135-148.
- Pantazopoulou, S.J. and French, C.W. (2001), “Slab participation in practical earthquake design of reinforced concrete frames”, *ACI Struct. J.*, **98**(4), 479-489.
- Park, Y.J. and Ang, A.H. (1985), “Mechanistic seismic damage model for reinforced concrete”, *J. Struct. Eng-ASCE*, **111**(4), 740-757.
- Prakash, V.G., Powell, H. and Campbell, S. (1993), “DRAIN-2DX Base program description and user guide”, Report UCB/SEMM-93/17, University of California at Berkeley.
- Priestley, M.J.N. (2000), “Performance based seismic design”, *Proceedings of the 12th World Conference on Earthquake Engineering*, New Zealand, January.
- Qi, X. and Moehle, J.P. (1991), “Displacement design approach for reinforced concrete structures subjected to earthquakes”, Report UCB/EERC-91/02, University of California at Berkeley.
- Reyes Salinas, C. (2000), *El estado limite de servicio en el diseño sísmico de edificios*, Doctoral Thesis, Universidad Nacional Autónoma de México.
- Rodríguez, M.E. and Botero, J.C. (1997), “Evaluación del comportamiento de barras de acero de refuerzo sometidas a cargas monotónicas y cíclicas reversibles incluyendo pandeo”, *Revista de Ingeniería Sísmica*, **56**, 9-27.
- Rodríguez, M.E. and Aristizabal, J.C. (1999), “Evaluation of a seismic damage parameter”, *Earthq. Eng. Struct. D.*, **28**, 463-477.
- SEAOC (1995), “Performance based seismic engineering of buildings”, Vision 2000 Committee.
- Seed, H.B. and Sun, J.I. (1989), “Implications of site effects in the Mexico City Earthquake of Sept.19, 1985 for earthquake-resistant design criteria in the San Francisco Bay Area of California”, Report No. UCB/EERC-89/03, University of California at Berkeley.
- Silva-Olivera, H. and Lopez-Batiz, O. (2001), “Estudio experimental sobre índices de daño en estructuras de concreto reforzado sujetas a cargas laterales”, *Proceedings of the 13th Mexican Conference on Earthquake Engineering*, Guadalajara, October.
- Teran-Gilmore, A. and Bertero, V.V. (1993), “Seismic performance of a 30-story building located on soft soil and designed according to UBC 1991”, Report No. UCB/EERC-93/04, University of California at Berkeley.
- Teran-Gilmore, A. (1996), *Performance-based earthquake-resistant design of framed buildings using energy concepts*, Doctoral Thesis, University of California at Berkeley.
- Teran-Gilmore, A. (1998), “Características mecánicas y desempeño sísmico de marcos dúctiles de concreto reforzado”, *Proceedings of the 11th Mexican Conference on Structural Engineering*.
- Teran-Gilmore, A. (2004), “On the use of spectra to establish damage control in regular frames during global pre-design”, *Earthq. Spectra*, **20**(3), 1-26.
- Teran-Gilmore, A. and Jirsa, J.O. (2005), “A Damage Model for Practical Seismic Design that Accounts for Low Cycle Fatigue”, *Earthq. Spectra*, **21**(3), 803-832.
- Teran-Gilmore, A. and Bahena-Arredondo, N. (2008), “Cumulative ductility spectra for seismic design of ductile structures subjected to long duration motions: concept and theoretical background”, *J. Earthq. Eng.*, **12**(1), 152-172.
- Williams, M.S. and Sexsmith, R.G. (1997), “Seismic assessment of concrete bridges using inelastic damage analysis”, *Eng. Struct.*, **19**(3), 208-216.